728385

Security Classification

DOCUMENT CONTROL DATA - R & D

(Security classification of title, body of abstract and indexing annotation must be entered when the overall report is classified)

Naval Research Laboratory Washington, D.C. 20390	Unclassified

CRACK PROPAGATION IN ALUMINUM ALLOYS UNDER HIGH-AMPLITUDE CYCLIC LOAD

DESCRIPTIVE NOTES (Type of report and inclusive dates): This report completes one phase; work continues on other phases of the problem.

AUTHOR(S) (First name, middle initial, last name):

T. W. Crooker

REPORT DATE	TOTAL NO. OF PAGES	NO. OF REFS
July 12, 1971	20	20

CONTRACT OR GRANT NO.	ORIGINATOR'S REPORT NUMBER(S)
NRL Problem M01-25 PROJECT NO. RR 007-01-46-5432	NRL Report 7286
c. d.	OTHER REPORT NO(S) (Any other numbers that may be assigned this report)

DISTRIBUTION STATEMENT

Approved for public release; distribution unlimited.

SUPPLEMENTARY NOTES	SPONSORING MILITARY ACTIVITY
	Department of the Navy (Office of Naval Research) Arlington, Va. 22217

ABSTRACT

Crack propagation studies were conducted on a variety of structural aluminum alloys under high stress-intensity amplitude cyclic load ($\Delta K > 10$ ksi $\sqrt{in.}$). The alloys under investigation included 2219-T87, 5456-H321, 6061-T651, 7005-T63, 7039-T6X31, and 7106-T63. The yield strengths of these alloys ranged from 34 to 55 ksi. Tests were conducted in ambient room air and in 3.5-percent NaCl saltwater environments. Data are presented on log-log coordinates in terms of fatigue crack growth rate (da/dN) as a function of the stress-intensity factor range (ΔK).

The air environment data plots for all of the alloys consist of two intersecting rectilinear curves, with the upper branch following a steeper slope. The point of transition between the two branches of the curves generally agreed well with predictions based on a crack-opening-displacement (COD) model for slope transition behavior in fatigue. Data along the lower branches of the curves for all of the alloys were similar and fell within a narrow scatterband. However, considerable disparity was observed among the upper branches of the curves, with the tougher alloys exhibiting superior crack propagation resistance. Comparisons among similar crack propagation data for steel and titanium alloys showed that each alloy family has a characteristic behavior pattern under high-amplitude cycling. Efforts to normalize this behavior on the basis of a universal crack propagation law can only be accomplished on a very broad basis.

(continues)

DD FORM 1 NOV 68 1473 (PAGE 1)

S/N 0101-807-6801

Security Classification

Security Classification

KEY WORDS	LINK A		LINK B		LINK C	
	ROLE	WT	ROLE	WT	ROLE	WT
Aluminum alloys Fatigue Corrosion fatigue Crack propagation Fracture mechanics Fracture toughness						

Among the alloys tested in a saltwater environment, only 7005-T63 was highly sensitive to saltwater under high-amplitude cyclic loading. Crack growth rates in alloys 2219-T87, 5456-H321, and 6061-T651 showed little or no sensitivity to saltwater under high-amplitude cycling.

DD FORM 1 NOV 65 1473 (BACK)

Security Classification

CONTENTS

ABSTRACT

Crack propagation studies were conducted on a variety of structural aluminum alloys under high stress-intensity amplitude cyclic load (ΔK = 10 ksi $\sqrt{in.}$). The alloys under investigation included 2219-T87, 5456-H321, 6061-T651, 7005-T63, 7039-T6X31, and 7106-T63. The yield strengths of these alloys ranged from 34 to 55 ksi. Tests were conducted in ambient room air and in 3.5-percent NaCl saltwater environments. Data are presented on log-log coordinates in terms of fatigue crack growth rate (da/dN) as a function of the stress-intensity factor range (ΔK).

The air environment data plots for all of the alloys consist of two intersecting rectilinear curves, with the upper branch following a steeper slope. The point of transition between the two branches of the curves generally agreed well with predictions based on a crack-opening-displacement (COD) model for slope transition behavior in fatigue. Data along the lower branches of the curves for all of the alloys were similar and fell within a narrow scatterband. However, considerable disparity was observed among the upper branches of the curves, with the tougher alloys exhibiting superior crack propagation resistance. Comparisons among similar crack propagation data for steel and titanium alloys showed that each alloy family has a characteristic behavior pattern under high-amplitude cycling. Efforts to normalize this behavior on the basis of a universal crack propagation law can only be accomplished on a very broad basis.

Among the alloys tested in a saltwater environment, only 7005-T63 was highly sensitive to saltwater under high-amplitude cyclic loading. Crack growth rates in alloys 2219-T87, 5456-H321, and 6061-T651 showed little or no sensitivity to saltwater under high-amplitude cycling.

PROBLEM STATUS

This report completes one phase of the problem; work on other aspects of the problem is continuing.

AUTHORIZATION

NRL Problem M01-25
Project RR 007-01-46-5432

Manuscript submitted April 7, 1971.

CRACK PROPAGATION IN ALUMINUM ALLOYS UNDER HIGH-AMPLITUDE CYCLIC LOAD

INTRODUCTION

High-performance structures frequently must be designed to withstand a finite number of repeated load applications in service. For such structures low-cycle fatigue is a potential failure mechanism. A significant portion of low-cycle fatigue life involves crack propagation, even in laboratory tests conducted on precision specimens which are initially polished and free of macroscopic defects (1,2). In actual structures, where there is a much greater probability that preexisting processing or fabrication defects will occur, nearly all low-cycle fatigue involves crack propagation. Therefore, designers of highly stressed critical structures are increasingly including crack propagation criteria in their fatigue design considerations. This new approach to fatigue design rests on the assumption that flaws, equivalent to the minimum defect size that can be reliably detected by nondestructive inspection methods, exist in critical regions of the structure prior to service, and that a lower-bound estimate for the fatigue life of the structure will depend on the growth of such flaws (3).

This report discusses fatigue crack propagation in a variety of intermediate- to high-strength aluminum alloys under high-amplitude elastic loading. Alloys of the 2000, 5000, 6000, and 7000 series with yield strengths from 34 to 55 ksi were investigated using the crack-tip stress-intensity factor range (ΔK) as the primary variable in describing crack growth rates. The ΔK values studied varied from approximately 12 to 50 ksi$\sqrt{\text{in.}}$ Tests were conducted in both ambient room air and saltwater environments. The results of this study provide a definitive materials characterization and are applicable as basic criteria for fatigue design.

MATERIALS

The alloys studied in this investigation included 2219-T87, 5456-H321, 6061-T651, 7005-T63, 7039-T6X31, and 7106-T63. All of the alloys, except 7039-T6X31, were received as 1-in.-thick rolled-plate stock. The 7039-T6X31 alloy was received as a 6-in.-thick rolled plate. The tensile properties of these alloys are shown in Table 1, and their fracture toughness characteristics are plotted on the NRL Ratio Analysis Diagram (RAD) (4) in Fig. 1.

As shown in Fig. 1, all of the 7000-series alloys studied lie on or near the current technological limit for maximum attainable fracture toughness, and are representative of the toughest alloys that are available at their respective yield strength levels. Three of the alloys, 5456-H321, 6061-T651, and 7005-T63, lie well above the K_{Ic}/σ_{ys} ratio line of 1.0, which indicates that they are incapable of fracturing without a significant amount of gross plastic deformation. Alloys 7039-T6X31 and 7106-T63 lie just below this unity ratio line, indicating that elastic instability fracture is possible in these alloys in section sizes several inches thick, if large flaws are present. Finally, alloy 2219-T87 lies just above the K_{Ic}/σ_{ys} ratio line of 0.5, which indicates that this alloy is capable of elastic instability fracture in section sizes down to approximately 1-in. thick in the presence of small flaws. Thus, these alloys represent a broad range in both strength and toughness properties.

Table 1
Tensile Properties

Alloy	0.2% Yield Strength (ksi)	Ultimate Tensile Strength (ksi)	Reduction of Area (%)	Elongation (%)
2219-T87	55	72	14	16
5456-H321	34	—	—	—
6061-T651	38	44	40	19
7005-T63	46	52	52	16
7039-T6X31	52	62	40	16
7106-T63	52	61	40	14

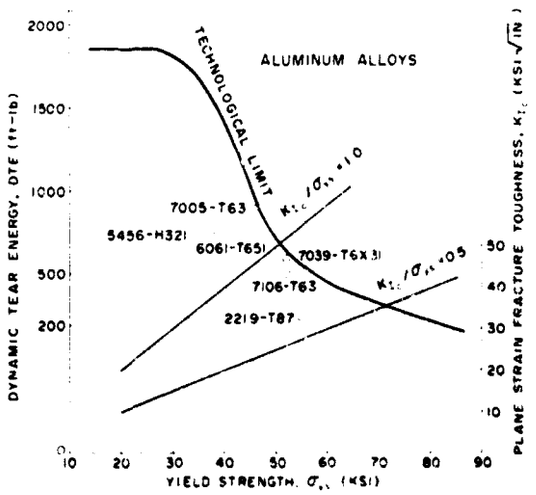

Fig. 1 - NRL RAD for aluminum alloys showing the fracture toughness characteristics of the alloys studied in this investigation

EXPERIMENTAL PROCEDURES

Crack propagation data were obtained using 0.5-in.-thick single-edge-notched (SEN) cantilever specimens cycled zero-to-tension under constant load at 6 cycles per minute. Details of the test specimen are shown in Fig. 2. Periodic crack-length measurements were made with an optical micrometer. Cracks were propagated to a maximum depth of 1.5 in. (a/w = 0.6) unless interrupted by fracture. Stress-intensity factors were calculated using Kies' (5) equation and were corrected for crack tip plasticity before final plotting (6). The crack-opening-displacement (COD) values reported are derived from calculations (7) and are not based on COD measurements.

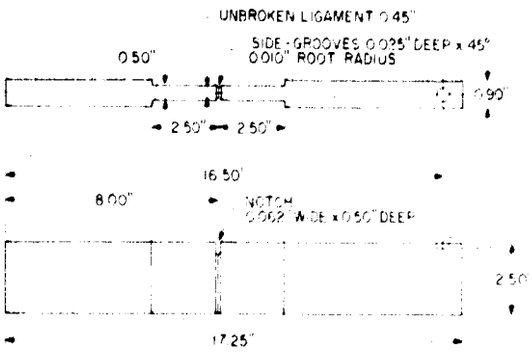

Fig. 2 - Crack propagation test specimen details

For tests involving a saltwater environment, a polyurethane corrosion cell is placed around the specimen test section. Distilled water containing 3.5-weight-percent NaCl is pumped through the cell on a continuous basis, with aeration and filtering included in the system. A plexiglass window in the cell permits optical observation of the crack.

RESULTS AND DISCUSSION

Basic Characteristics

Figures 3 through 8 are log-log plots of da/dN versus ΔK, which define the basic crack propagation characteristics of the aluminum alloys investigated. These data were obtained in ambient room air and are considered to be baseline curves for comparisons among various alloys and for establishing environmental effects.

Each of the curves in Figs. 3 through 8 consists of two rectilinear branches with a distinct point of slope transition in midregion. Each of the two branches can be defined by a power-law relationship of the form

$$da/dN = C(\Delta K)^m, \tag{1}$$

where da/dN is the fatigue crack growth rate (in./cycle), ΔK is the stress-intensity factor range (ksi $\sqrt{\text{in.}}$), and C and m are constants. Data forming the lower branches tend to be rather closely grouped within a narrow scatterband, as shown in the summary data plot in Fig. 9. However, above the slope transition region, the upper branches of the curves are more widely separated, with the tougher alloys generally occupying the more favorable portion of the scatterband. Similar findings have been reported in a separate investigation of fatigue crack propagation in high-strength aluminum alloys (8). The most favorable characteristics in this region were exhibited by the 7000-series alloys. However, because of higher yield strengths in the 7000-series alloys leading to higher anticipated working stresses, this advantage does not necessarily translate into superior fatigue performance in actual structural service (9).

The point of slope transition for each alloy generally agreed quite well with a COD model proposed by Barsom (7). Previous studies have shown broad agreement between this model and a wide variety of aluminum, steel, and titanium alloys (7,10,11). Barsom's model proposes that slope transition behavior is related to a change in the microfracture mode from exclusive striation formation to a mixture of striations and microvoid coalescence (12). Observation has shown that this point can be predicted on the basis of a constant

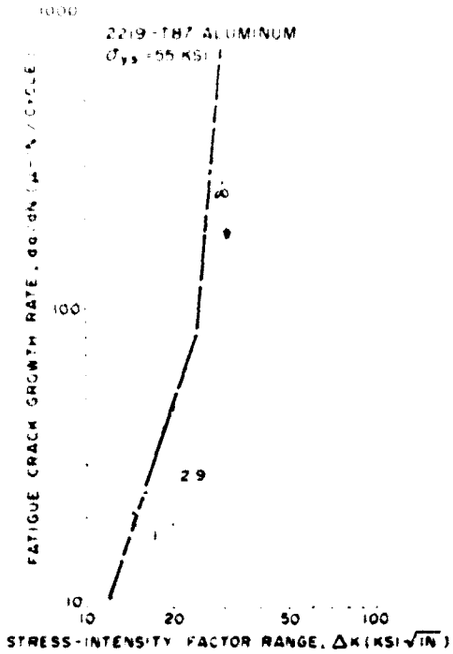

Fig. 3 - Log-log plot of fatigue crack growth rate (da/dN) as a function of stress-intensity factor range (ΔK) for 2219-T87 aluminum in an ambient room air environment

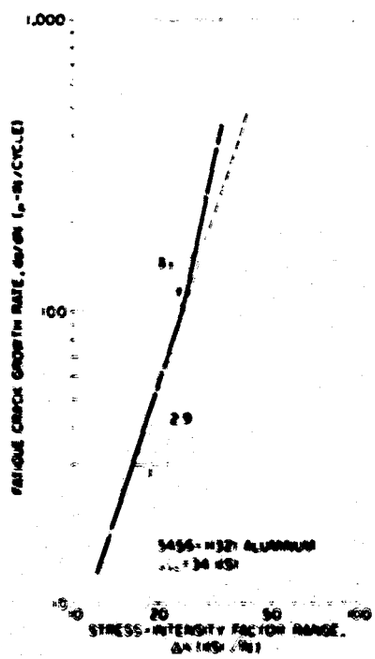

Fig. 4 - da/dN versus ΔK data for 5156-H321 aluminum in air

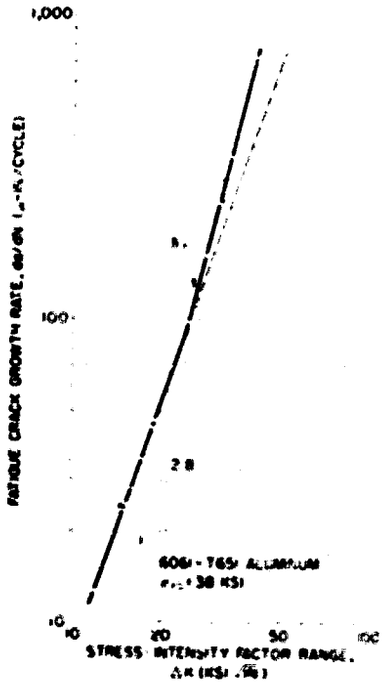

Fig. 5 - da/dN versus ΔK data for 6061-T651 aluminum in air

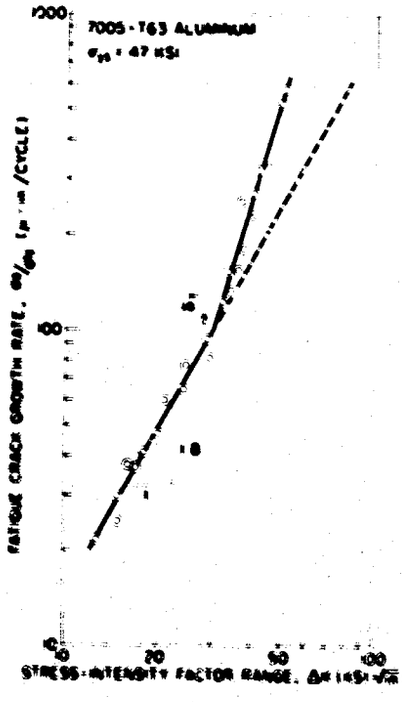

Fig. 6 - da/dN versus ΔK data for 7005-T63 aluminum in air

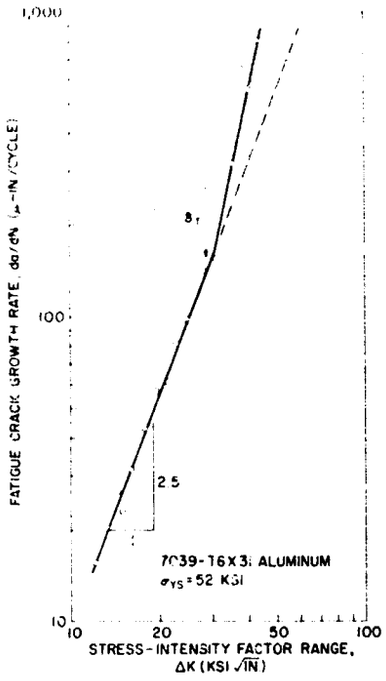

Fig. 7 - da/dN versus ΔK data for 7039-T6X31 aluminum in air

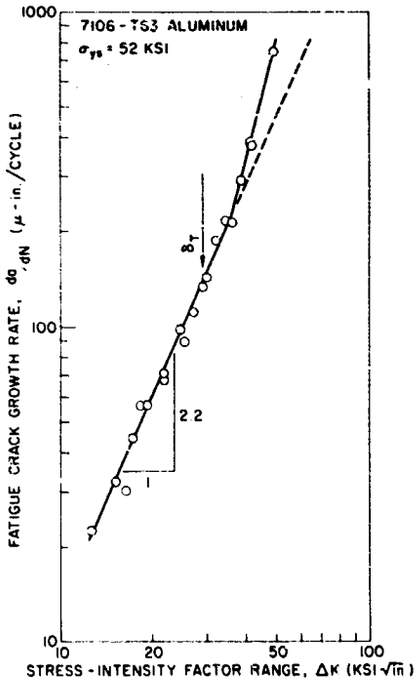

Fig. 8 - da/dN versus ΔK data for 7106-T63 aluminum in air

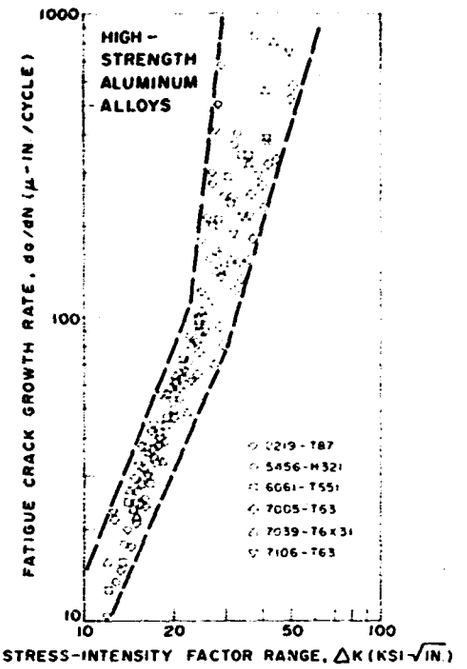

Fig. 9 - Summary plot of da/dN versus ΔK data for the six aluminum alloys studied in this investigation. The yield strengths of these alloys range from 34 to 55 ksi.

COD value (7). The COD expression as derived by Wells (13) is given by

$$\delta = \mathcal{J}/\sigma_{ys}, \tag{2}$$

where δ is the COD (in.), $\mathcal{J}$ is the strain energy release rate (ksi-in.), and σ_{ys} is the 0.2-percent yield strength stress (ksi). By applying the relationship between $\mathcal{J}$ and K in plane stress,

$$\mathcal{J} = (1/E)K^2, \tag{3}$$

δ can be expressed as a function of K:

$$\delta = K^2/E\sigma_{ys}. \tag{4}$$

Denoting the constant value of COD at the transition point as δ_T, the corresponding ΔK_T value can be calculated for various materials from

$$\Delta K_T = \sqrt{\delta_T E \sigma_{ys}}, \tag{5}$$

where δ_T is a constant and E is Young's Modulus (ksi). The calculated value of ΔK corresponding to δ_T is shown for each material in Figs. 3 through 8, using a value of 0.0016 in. for δ_T (7).

Agreement between Barsom's COD model and the experimental data is generally excellent, the most notable exceptions being alloys 2219-T87 and 7106-T63. The slope transition behavior of 7106-T63 appears to be anomalous, and the difference between the actual and the predicted values of ΔK for this alloy is relatively small. However, for alloy 2219-T87 a different set of circumstances prevails. This is the highest-strength, lowest-toughness material studied in this investigation, and it is recognized that the COD slope transition model is only applicable to higher-toughness alloys where slope transition behavior is not related to the onset of elastic instability fracture. The COD model predicts

that ΔK_T will increase in proportion to $\sqrt{\sigma_{ys}}$. However, this process can only proceed to the point where ΔK_T approaches the fracture toughness (K_c or K_{Ic}) of the material. Beyond that strength level, the COD model is no longer valid. In the case of alloy 2219-T87, the COD model predicted a value of ΔK_T beyond the ΔK level where brittle fracture occurred. Despite this limitation, the model has been remarkably accurate in predicting the behavior of a wide variety of alloys under a broad range of experimental conditions. A summary tabulation of the slope, intercept, and slope-transition constants for these alloys is shown in Table 2.

Table 2
Slope, Intercept, and Slope-Transition Constants

Alloy	Lower Branch		Upper Branch		Slope Transition	
	Intercept C_1	Slope m_1	Intercept	Slope m_2	Calculated ΔK_T	Actual ΔK_T
2219-T87	7.97×10^{-9}	2.9	5.24×10^{-20}	11.0	30.5	24.0
5456-H321	8.83×10^{-9}	2.9	3.81×10^{-11}	4.6	24.0	25.0
6061-T651	1.21×10^{-8}	2.8	2.67×10^{-10}	4.0	25.5	24.5
7005-T63	2.19×10^{-7}	1.8	1.36×10^{-9}	3.3	28.0	30.0
7039-T6X31	3.04×10^{-8}	2.5	2.14×10^{-11}	4.6	29.0	31.0
7106-T63	8.42×10^{-8}	2.2	2.91×10^{-10}	3.8	29.0	36.0

The significance of slope transition behavior can be very important in low-cycle fatigue. To ignore such behavior and simply extrapolate the lower branch of the curves in Figs. 3 through 8 out to an estimated K_{Ic} value would seriously overestimate fatigue life. This has been discussed by Carman and Katlin (14) for the case of ultrahigh-strength steels, but it is not generally recognized that many intermediate-strength ductile alloys exhibit similar slope transition behavior at ΔK levels well below K_{Ic}. Accurate prediction of finite fatigue life in the low-cycle region (less than 100,000 cycles to failure) cannot be based on extrapolated data and requires a definitive characterization of fatigue behavior under high-amplitude cycling.

Comparisons Among Alloy Families

A summary plot of all the da/dN versus ΔK data obtained in this investigation is shown in Fig. 9. It is interesting to compare these data with similar plots for steel and titanium alloys. Figure 10 is a plot of da/dN versus ΔK data obtained from NRL studies for several steels ranging in yield strength from 175 to 250 ksi, and Fig. 11 shows similar data for titanium alloys ranging in yield strength from 110 to 150 ksi. Figure 12 shows scatterband limits for all three alloy families.

A number of researchers (7,15,16) have suggested that the crack propagation characteristics of all alloys fall within a single scatterband when ΔK is normalized with respect to Young's Modulus ($\Delta K/E$). Figure 12 suggests that this is possible for the case of high-amplitude cycling in a very broad sense only. However, normalizing the data represented in Fig. 12 would cause the scatterbands to overlap to a greater degree, but significant differences would persist. Crack propagation curves for high-strength titanium alloys typically follow much steeper slopes than for high-strength steels (17), and the aluminum

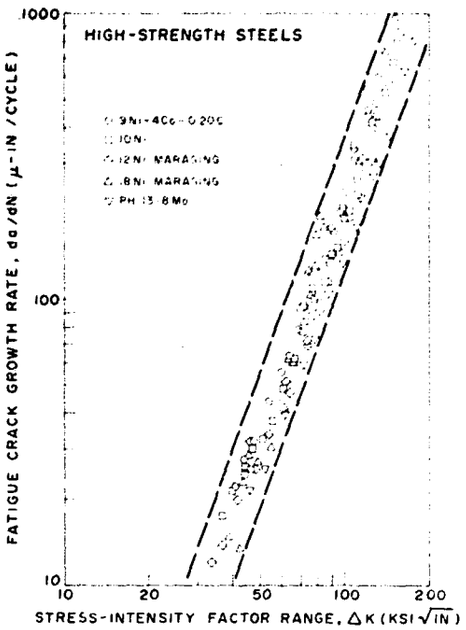

Fig. 10 - Summary plot of da/dN versus ΔK data for five steels ranging in yield strength from 175 to 250 ksi

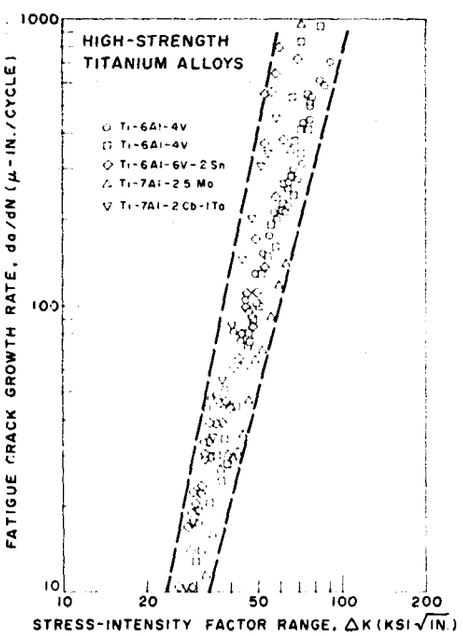

Fig. 11 - Summary plot of da/dN versus ΔK data for five titanium alloys ranging in yield strength from 110 to 150 ksi

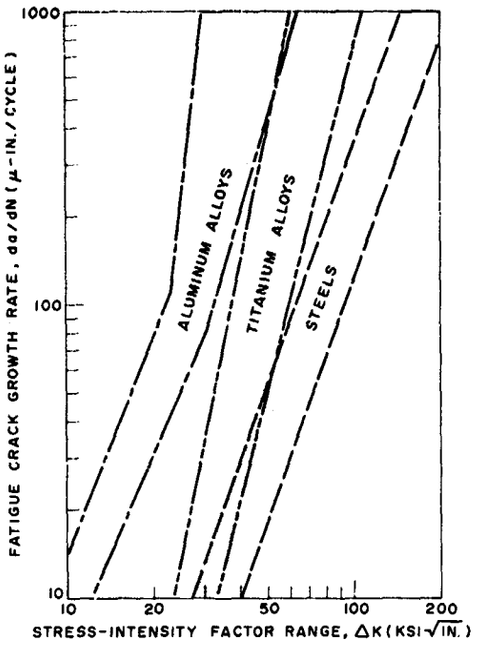

Fig. 12 - Scatterband limits for data on steel, titanium, and aluminum alloys from Figs. 9 through 11

alloys studied in this investigation have very pronounced slope transition behavior. These alloy family characteristics are reflected by the scatterbands in Fig. 12. Efforts to develop a universal crack propagation law for all materials must reconcile these various alloy family characteristics in order to offer accurate validity.

Environmental Sensitivity

Four of the alloys included in this investigation, 2219-T87, 5456-H321, 6061-T651, and 7005-T63, were studied under corrosion-fatigue crack propagation in 3.5-percent NaCl saltwater. Among these alloys, only 7005-T63 had previously been found to be sensitive to saltwater stress-corrosion cracking (SCC). Among the three 7000-series alloys studied, 7005-T63 was found to be the least sensitive to saltwater SCC (18,19). The K_{Iscc} threshold stress-intensity levels for saltwater SCC to occur in these 7000-series alloys is given in Table 3. Aluminum alloys are only susceptible to SCC in the short transverse (TW) orientation. The K_{Iscc} values reported above were taken in the TW orientation. However, all fatigue crack propagation tests, including corrosion fatigue, were conducted on specimens where the crack propagated in the long transverse (RW) orientation. Therefore, no direct correlation between these SCC characteristics and corrosion-fatigue crack propagation was anticipated.

Table 3
K_{Iscc} Values for 7000-Series Alloys

Alloy	K_{Iscc} (ksi $\sqrt{in.}$)
7005-T63	27.5
7039-T6X31	11.5
7106-T63	23.0

Corrosion-fatigue crack propagation data for the four alloys are shown in Figs. 13 through 16. Among these alloys only 7005-T63 exhibited a high degree of environmental sensitivity, as indicated by the displacement of the saltwater environment data above the baseline air environment data curve, Fig. 16. The remaining alloys showed much lesser degrees of

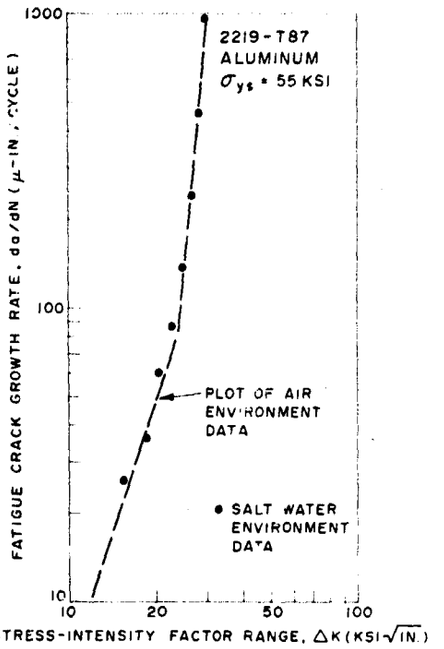

Fig. 13 - da/dN versus ΔK data for 2219-T87 aluminum in a 3.5-percent NaCl saltwater environment. The dashed line refers to the air environment data curve, Fig. 3.

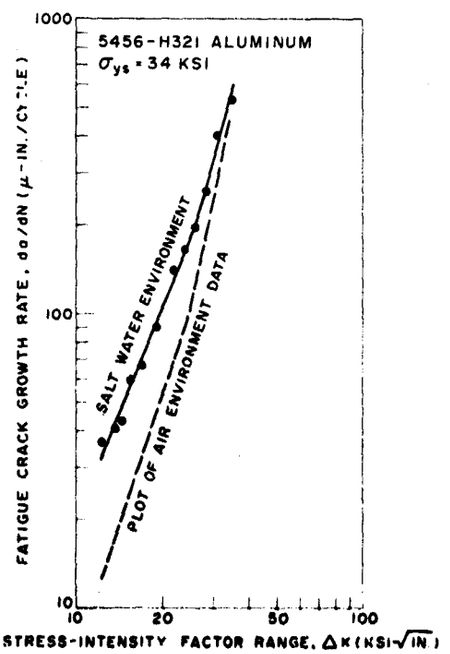

Fig. 14 - da/dN versus ΔK data for 5456-H321 aluminum in saltwater

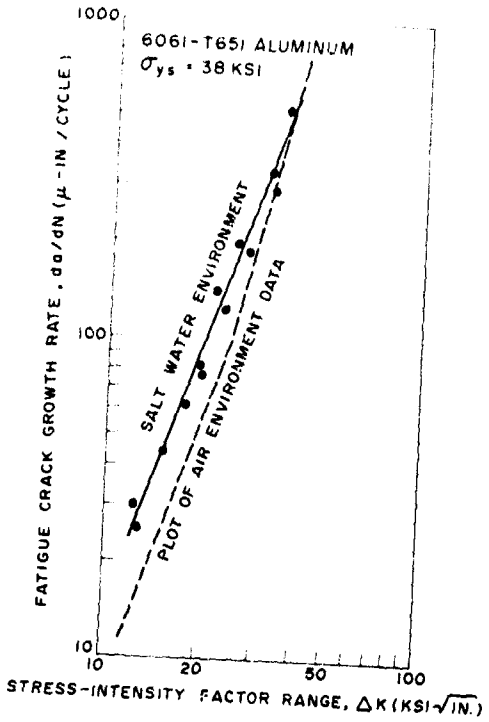

Fig. 15 - da/dN versus ΔK data for 6061-T651 aluminum in saltwater

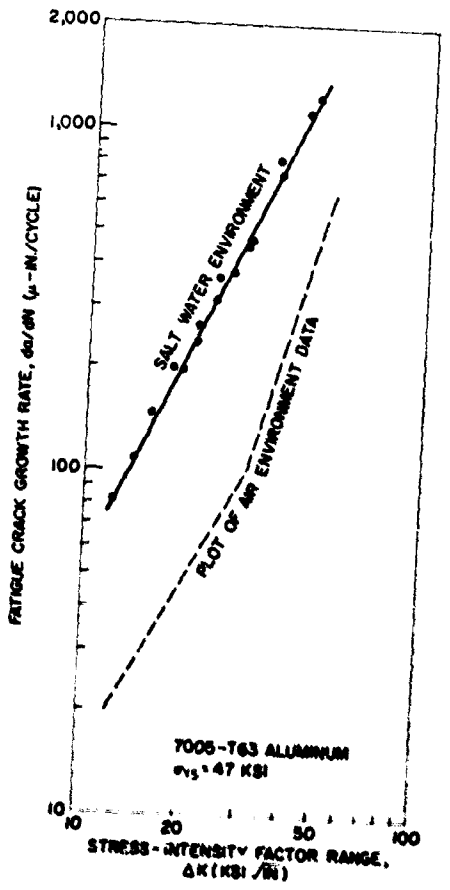

Fig. 16 - da/dN versus ΔK data for 7005-T63 aluminum in saltwater

environmental sensitivity, although none of the alloys, except 2219-T87 in Fig. 13, appeared to be completely unaffected by the saltwater environment.

These results for corrosion-fatigue crack propagation are in general agreement with recent studies (8,20). Nordmark and Kaufman (8) studied crack propagation in a wide variety of thick-section 2000- and 7000-series alloys in several environments. They reported that SCC-sensitive alloys showed the largest effects from humid and salt-spray environments. Feeney, et al. (20) studied environmental fatigue crack propagation in 2024-T3 and two 7000-series alloys in sheet thicknesses. Their findings showed the 7000-series alloys to be more environmentally sensitive than 2024-T3. They also showed that environmental effects were more pronounced under low-amplitude cycling ($\Delta K < 10$ ksi$\sqrt{\text{in.}}$). They related environmental sensitivity in aluminum alloys to crack tip stress state; i.e., reduced environmental sensitivity was observed at higher ΔK levels where plane-strain conditions cannot prevail. Their findings suggest that the modest degree of environmental sensitivity seen in alloys 2219-T87, 5456-H321, and 6061-T651 under high-amplitude cycling may not remain in thicker sections under plane strain conditions. However, pending evidence to the contrary, the saltwater corrosion-fatigue crack propagation characteristics of alloys 2219-T87, 5456-H321, and 6061-T651 are very encouraging.

CONCLUSIONS

The following conclusions have been reached from this investigation:

1. Log-log plots of fatigue crack growth rate (da/dN) versus stress-intensity factor range (ΔK) data for all of the alloys studied consist of two rectilinear curves meeting at a distinct point of slope transition. For most of the alloys, the point of slope transition agrees very accurately with predictions based on a crack-opening-displacement (COD) model for slope transition behavior.

2. A summary plot of da/dN versus ΔK for all of the alloys investigated shows that the lower branches of the respective curves all fall within a narrow scatterband with no apparent significant differences. However, above the region of slope transition, the upper branches of the curves are more widely separated with the higher-toughness alloys generally exhibiting the greatest crack propagation resistance.

3. Comparisons between the scatterband of da/dN versus ΔK for these aluminum alloys and similar scatterbands for steel and titanium alloys, also obtained under high-amplitude cycling, reveal distinct crack propagation characteristics for each family of alloys. The differences in crack propagation behavior among the various families of alloys suggest that efforts to fit all data into a universal crack propagation law can only be accomplished on a very approximate basis in the high-amplitude crack propagation regime.

4. Environmental effects of 3.5-percent NaCl saltwater on crack propagation were greatest in a 7000-series, stress-corrosion-cracking sensitive alloy. Environmental effects were modest or nil in the 2000-, 5000-, and 6000-series alloys examined.

ACKNOWLEDGMENTS

The author acknowledges the contributions of R.J. Hicks and M.L. Cigledy, who conducted the fatigue testing, and the Office of Naval Research for their financial support of this work.

REFERENCES

1. J.C. Grosskreutz, "Fatigue Mechanisms and the Development of Fatigue-Resistant Materials," Proc., Air Force Conference on Fatigue and Fracture of Aircraft Structures and Materials, Miami Beach, Florida, Dec. 15-18, 1969, p. 47 (also, Air Force Materials Laboratory Technical Report AFML-TR-70-55, May 1970)

2. R.C. Boettner, C. Laird, and A.J. McEvily, Jr., "Crack Nucleation and Growth in High Strain-Low Cycle Fatigue," Trans. Met. Soc. AIME 233, 379 (1965)

3. W.G. Clark, Jr., "Fracture Mechanics and Nondestructive Testing," Westinghouse Scientific Laboratories Paper 70-1E7, MSLRF-P2, July 20, 1970; also ASME Paper 71-PVP-4

4. R.W. Judy, Jr., R.J. Goode, and C.N. Freed, "Fracture Toughness Characterization Procedures and Interpretations to Fracture-Safe Design for Structural Aluminum Alloys," NRL Report 6871, Mar. 31, 1969

5. J.A. Kies, et al., "Fracture Testing of Weldments" in Fracture Toughness Testing and Its Applications, ASTM STP 381, American Society for Testing and Materials, 1965, p. 328

6. P.C. Paris, "The Fracture Mechanics Approach to Fatigue" in Fatigue-An Interdisciplinary Approach, Proceedings 10th Sagamore Army Materials Research Conference, Aug. 13-16, 1963, Syracuse University Press, 1964, p. 107

7. J.M. Barsom, "The Dependence of Fatigue-Crack Propagation on Strain-Energy Release Rate and on Crack-Opening Displacement," to be published in ASTM STP 486

8. G.E. Nordmark and J.G. Kaufman, "Fatigue-Crack Propagation Characteristics of Aluminum Alloys in Thick Sections," Alcoa Research Laboratories Report 12-70-23 and 9-M-885, Sept. 14, 1970

9. T.W. Crooker, "Structural Interpretation of Fatigue Crack Propagation in Aluminum Alloys," Report of NRL Progress, Mar. 1971

10. J.M. Barsom, "Fatigue-Crack Propagation in a Range of Steels," ASME Paper 71-PVP-12

11. T.W. Crooker, "Slope Transition Behavior of Fatigue Crack Growth Rate Curves," Report of NRL Progress, Dec. 1970, pp. 25-27

12. W.G. Clark, Jr. and E.T. Wessel, "Interpretation of the Fracture Behavior of 5456-H321 Aluminum with WOL Toughness Specimens," Westinghouse Research Laboratories Scientific Paper 67-106-BTLFR-P4, Sept. 8, 1967

13. A.A. Wells, "Notched Bar Tests, Fracture Mechanics and the Brittle Strengths of Welded Structures," Brit. Welding J. 12, No. 1, 2 (1965)

14. C.M. Carman and J.M. Katlin, "Low Cycle Fatigue Crack Propagation Characteristics of High Strength Steels," Am. Soc. Mech. Engrs. Trans. J. Basic Eng. 88, Series D, No. 4, 792 (1966)

15. D.R. Donaldson and W.E. Anderson, "Crack Propagation Behaviour of Some Airframe Materials," Proc. Crack Propagation Symp., Cranfield, England, 2, 375 (1961)

16. R.C. Bates and W.G. Clark, Jr., "Fractography and Fracture Mechanics," ASM Trans. Quart. 62, No. 2, 380 (1969)

17. T.W. Crooker and E.A. Lange, "Effects of a 3.5 Per Cent Sodium Chloride Aqueous Saline Environment on the Fatigue Crack Propagation Characteristics of Titanium Alloys," Applications Related Phenomena in Titanium Alloys, ASTM STP 432, American Society for Testing and Materials, 1968, p. 251

18. P.P. Puzak, et al., "Metallurgical Characteristics of High Strength Structural Materials," NRL Report 6513 (Eleventh Quarterly Report), Aug. 1966

19. R.J. Goode, et al., "Metallurgical Characteristics of High Strength Structural Materials," NRL Report 6607 (Twelfth Progress Report), Sept. 1967

20. J.A. Feeney, J.C. McMillan, and R.P. Wei, "Environmental Fatigue Crack Propagation of Aluminum Alloys at Low Stress Intensity Levels," Metallurgical Trans. 1, 1741 (1970)